HAL open science

Influence of the geopolymer formulation on the endogeneous shrinkage

Julien Archez, Rémi Farges, Ameni Gharzouni, Sylvie Rossignol

To cite this version:

Julien Archez, Rémi Farges, Ameni Gharzouni, Sylvie Rossignol. Influence of the geopolymer formulation on the endogeneous shrinkage. Construction and Building Materials, 2021, 298, pp.123813. 10.1016/j.conbuildmat.2021.123813 . hal-03402198

HAL Id: hal-03402198

https://unilim.hal.science/hal-03402198v1

Submitted on 13 Jun 2023

HAL is a multi-disciplinary open access archive for the deposit and dissemination of scientific research documents, whether they are published or not. The documents may come from teaching and research institutions in France or abroad, or from public or private research centers.

L'archive ouverte pluridisciplinaire **HAL**, est destinée au dépôt et à la diffusion de documents scientifiques de niveau recherche, publiés ou non, émanant des établissements d'enseignement et de recherche français ou étrangers, des laboratoires publics ou privés.

Distributed under a Creative Commons Attribution - NonCommercial 4.0 International License

Version of Record: https://www.sciencedirect.com/science/article/pii/S0950061821015737
Manuscript_72204dbec09b8f5529727f09d3653c3f

INFLUENCE OF THE GEOPOLYMER FORMULATION ON THE ENDOGENEOUS SHRINKAGE

Julien Archez, Rémi Farges, Ameni Gharzouni, Sylvie Rossignol

IRCER: Institut de Recherche sur les Céramiques (UMR7315), 12 rue Atlantis, 87068 Limoges Cedex, France.

■ Corresponding author: sylvie.rossignol@unilim.fr, tel.: 33 5 87 50 25 64

Geopolymer	Endogenous	Shrinkage
Alkaline solution	Metakaolin	Sand

Abstract

The shrinkage of geopolymer materials is an important parameter to control for several applications. In this topic, this study aims to investigate the role of used precursors (metakaolin and alkaline solution) and different additives (sand, normalized sand, wollastonite, and glass fibers) on the shrinkage. For this, different samples were synthesized and stored at 20°C and 100% RH. Then, shrinkage measurements were carried out at different consolidation times. The results have shown that the measured shrinkage is endogenous because it is not accompanied by mass variation and is only due to self-desiccation. It was also evidenced that the used alkaline solution controls the shrinkage. In fact, the increase of alkalinity or the use of sodium instead of potassium solutions permits to decrease the shrinkage values to less than 400 µm/m at 28 days. This result is explained by different depolymerization degrees of the solution inducing different geopolymerization rates and kinetics and affecting the pore distribution size. The metakaolin seems to have a lower impact on the shrinkage. The effect of additives was also studied. All additives reduce the shrinkage with different extents in the following order: normalized sand > sand > glass fiber > wollastonite. The normalized sand has shown the highest reduction of shrinkage (about 142 µm/m at 7 days) which can be explained by a modification of the granular skeleton and the

© 2021 published by Elsevier. This manuscript is made available under the CC BY NC user license
https://creativecommons.org/licenses/by-nc/4.0/

porosity. A correlation was proven to show the increase of the shrinkage with the increase of liquid to solid ratio.

I. INTRODUCTION

Geopolymers are inorganic materials synthesized by activation of an aluminosilicate source using an alkaline silicate solution at atmospheric pressure and below 100 ° C [1]. Unlike hydrated calcium silicate gel (CSH), formed during the hydration of Portland cement, geopolymers are composed of an amorphous three-dimensional aluminosilicate network based on SiO_4 and AlO_4 tetrahedral groups. Geopolymers have a lower environmental impact than Portland cement, which produces between 5 and 8 % of global CO_2 emissions [2, 3]. Geopolymers can for instance be used in the building industry, for the construction of airstrips [4] or fire-resistant applications [5]. They exhibit high compressive strengths, low thermal conductivity as well as resistance to high temperature and chemical aggressions (acids) [6, 7].

Studying the shrinkage of room temperature consolidating materials is crucial. The shrinkage can indeed induce the initiation and propagation of microcracks reducing the sealing and durability of the structure [8, 9]. The shrinkage mechanisms have been widely studied in the literature in the context of Portland cement [10,11] and are mainly caused by (i) chemical reaction during hydration, (ii) the variation of the water content in the cement paste, and (iii) by the environment (relative humidity and temperature). The Portland cement shrinkage can be decomposed in five mechanisms that follow each other or occur simultaneously: the plastic shrinkage induced by water loss due to evaporation; the thermal shrinkage due to strongly exothermic hydration reactions; the chemical shrinkage caused by hydration (Le Chatelier contraction); the desiccation shrinkage (or drying shrinkage) where a variation in the water content, caused by an imbalance between the initial humidity of the material and the external environment, generates a contraction of the matrix; the endogenous shrinkage or (auto-desiccation shrinkage) produced in the absence of any water exchange with the external environment caused by the hydration kinetics of the cement. Few studies have been carried out in the literature concerning geopolymer binders shrinkage. Li et al., [12] studied the chemical shrinkage of the geopolymers during their formation and observed three steps (shrinkage-expansion-shrinkage). Kuenzel et al., [13] studied the drying shrinkage of geopolymer compositions ($3.2 \leq SiO_2/Al_2O_3 \leq 4.8$; $0.7 \leq Na_2O/Al_2O_3 \leq 1.3$ and $7.5 \leq H_2O/Al_2O_3 \leq 10.5$) and concluded that, under low relative humidity conditions, the evaporation of the geopolymer structural water induces high capillary pressures between the wet and dry areas of the micropore network. The capillary pressure induces then a contraction

of the network and a shrinkage or even cracking of the material. To limit this phenomenon, Hawa et al., [14] have inserted palm oil that refines pores and decreases the shrinkage of geopolymers. Si et al., [15] have also shown that the addition of glass powder refines pores and limit the water loss, the capillary forces, and the shrinkage of geopolymers. Kuenzel et al., [16] and Rihai et al., [17] substituted metakaolin with sand. They showed that decreasing the amount of geopolymer in a given volume decreases shrinkage. Yang et al. [18] studied the endogeneous shrinkage (specimens wrapped in polyethylene film) and the drying shrinkage (50% HR, 25 °C) of a metakaolin-based geopolymer with the addition of different ratio of fly ashes. The composition containing only metakaolin present endogenous shrinkage values around 100 µm/m, linked to the loss of relative humidity during self-desiccation. This composition presented higher drying shrinkage values (6000 µm/m) that underline the impact of storage conditions. However, in the case of geopolymers, endogenous shrinkage can not only be explained by the theory of self-desiccation of Portland cement [12]. The dependence of the shrinkage and relative humidity was also highlighted. **Figure 1** regroups some shrinkage values, from literature, according to the relative humidity of storage for concrete at 60 % HR [19] or 100 % HR [20], alkali-activated material at 50-60 % [21, 22, 23, 24], 70-90 % HR [25, 26, 27, 28] or 100 % HR [29] and geopolymers at 45-50 % HR [18, 30, 31] and 100% HR [18]. It has been shown that the addition of sand [16, 17] or fibers [15] could decrease the shrinkage. The sand particles limit shrinkage by modifying the granular skeleton and forming a supportive network [16]. The sand can act as reinforcement in the geopolymer matrix and prevent crack growth. However, some applications like the elaboration of grouts [32], foams [33] or fire-resistant material [34] require the use of only binder formulations. Therefore, the formulation of the binder has to be studied to decrease the shrinkage.

The objective of the current study is to analyze the evolution of the endogenous shrinkage over time for different geopolymer formulations. For this, the influence of the used precursors (alkaline solutions and metakaolins) was at first studied. Then, the effect of different additives such as sand, normalized sand, wollastonite, and glass fibers has been investigated.

II. EXPERIMENTAL PART

1. Raw materials and samples preparation

The commercial alkali silicate solutions are supplied by Woellner. Alkali hydroxide pellets (MOH with M = Na or K) are used to adjust the alkali concentration. The solutions noted K^6, K^7, and K^9 are potassium silicates with alkali concentrations equal to 6, 7, and 9

mol. L^{-1}, respectively. The solution noted Na^9 is a sodium silicate with alkali concentrations equal to 9 mol. L^{-1}. The metakaolins are noted M1 (Si/Al = 1.17, D_{50} = 10 µm) and M5 (Si/Al= 1.46, D_{50}= 20 µm) and supplied by Imerys and Argeco respectively. Four additives were used in this study: (i) alkali-resistant glass fibers noted G and produced by Owens Coming (L = 6 mm, D = 13-15 µm), (ii) wollastonite noted W and supplied by Imerys (L = 5-170 µm, D = 3-15 µm), (iii) normalized sand denoted NS and supplied by "Société Nouvelle du Littoral" (CEN EN 196-1) and (iv) silica sand denoted S and supplied by Sibelco (D_{50} = 250 µm). A CEM I 52.5R white cement supplied by AXTON (D_{50} = 15 µm) was used to make mortar test pieces from normalized sand.

The synthesis protocol for the geopolymer samples is presented in **Figure 2**. Alkali hydroxide pellets are dissolved in the alkali silicate solution to adjust the Si/M molar ratio. The metakaolin is then gradually added to the alkaline solution and the whole is mixed until the homogenization of the mixture. Additives are then added and mixed for 10 min. The weight percentage of the different additives is detailed in **Table 1**. The obtained reactive mixture is poured into 4 x 4 x 16 cm prismatic molds made of elastomer. The molds are fitted with stainless steel inserts and allow the obtaining of three specimens to carry out the shrinkage measurement according to NF P15-433 standard (**Figure 3a**). The samples are unmolded after 24 hours and stored in plastic bags at a temperature of 20 °C and a relative humidity of 100% (**Figure 3b**). The samples are denoted as C^xMyA (**Table 1**), with C refers to the alkali cation C=K or Na and x the alkali cation concentration x=6, 7 or 9, "My" refers to metakaolin My=M1 or M5 and A denotes the used additive with A= G, W, S or NS. For example, K^7M1NS is a geopolymer based on a potassium alkaline solution with an alkali concentration of 7 mol.L^{-1}, metakaolin M1 and normalized sand as additive.

2. Sample characterization

Differential thermal analysis (DTA) and thermogravimetric analysis (TGA) were performed with a SDT Q600 apparatus from TA Instruments, in an atmosphere of flowing dry air (100 mL/minute) in platinum crucibles. The signals were measured with Pt/Pt–10%Rh thermocouples. A fragment of the sample (m = 30 mg) was heated up to 300°C with a rate of 5°C/min.

The open porosity was calculated using Archimedes' method following NF EN 623-2 standard. Samples were previously dried at 90°C.

The shrinkage measurements are carried out with a Proviteq deformometer according to NF P15-433 standard (**Figure 3a**). Before each measurement, the device is calibrated by placing a 160 mm invar® rod between two 4 mm stainless steel balls. The shrinkage is calculated according to **Equation 1** and the device error is 1 µm. The shrinkage values, expressed in µm/m is the average of three samples. For each shrinkage measurement, the samples are weighed using a Denver Instrument SI-603 precision balance (error = 0.001 g).

$$\text{Shrinkage } (\mu m/m) = \frac{L(t0) - L(t)}{0.160} \quad (\textbf{Equation 1})$$

with L(t0) (µm) the length of the sample directly after demolding (t0) and L(t) (µm), the length of the sample at time t.

The mechanical strength was measured by compressive tests using an Instron 5969 with a 50 kN load cell at a constant speed of 0.5 $mm.min^{-1}$, and was measured after seven days on six cylindrical samples, with a 15 mm diameter and a 30 mm height.

Environmental Scanning Electron Microscopy experiments were conducted using a FEI QUANTA 450 FEG microscope at 15 kV. The geopolymer sample was directly placed in a small MgO crucible covered with a platinum paint (5 mm inner diameter). The thermocouple is placed below the sample. The temperature was increased from 25 to 300°C (step=25°C). The pressure is maintained at 200 Pa. Many images of the sample surface were recorded during the temperature variation.

III. Results and Discussion

1. Identification of the shrinkage type

Figure 4a shows the shrinkage evolution over time of the sample K^6M1 stored at 100 % RH and 20 °C. A continuous increase in the shrinkage over time is noticed. At 28 days, the shrinkage reaches 1350 µm/m. In order to identify the type of the measured shrinkage (endogenous or drying), the variation of the mass as a function of the time is plotted in **Figure 4b**. The results show that the variation in mass is very small and does not change over time which means that the shrinkage is caused by the self-desiccation due to water consumption in geopolymerization reactions and not to a water departure by evaporation [35, 36]. In order to confirm this result, thermal analyses (DTA-DTG) were carried out. Mass losses typical of geopolymer materials and attributed to the release of free, adsorbed, and structural water were detected [37]. The evolution of the total mass loss of K^6M1sample stored at 100 % RH as a function of time is plotted in **Figure 4b**. The total weight loss value is equal to 40 % and

remains constant over time, which confirms that there is no drying of the sample. The small mass loss variations observed may be due to the device error which is approximately equal to 1 %. Thus, the measured shrinkage in the study conditions is endogenous.

2. Impact of precursors on the endogenous shrinkage

In order to assess the effect of the alkaline solution and the metakaolin on the shrinkage, different geopolymer formulations have been synthesized with two metakaolins (M1 and M5) and three alkaline solutions having different alkali-cation type (M= Na or K) and concentrations [M]=6 or 9 mol.L^{-1} (**Table 1**). The samples were stored under the same conditions detailed previously. The evolution of the shrinkage of the different samples as a function of time is presented in **Figure. 5 A**. Whatever the sample, the shrinkage increases over time. However, differences can be observed depending on the alkaline solution and metakaolin used. On one hand, for the same metakaolin M1, samples based on potassium solutions (K^6 and K^9) exhibit similar shrinkage evolution curves and higher shrinkage than sodium-based samples. The shrinkage values at 28 days are about 1350, 1200, and 400 µm/m for K^6M1, K^9M1, and Na^9M1 samples, respectively. Furthermore, the kinetic of shrinkage increase is low until 7 days and more important until 28 days. This is not the case for Na^9M1 sample which shows a low kinetic of shrinkage increase over 28 days.

On the other hand, for samples based on metakaolin M5, K^6M5 sample exhibits the highest shrinkage value whatever the time of measurement while K^9M5 sample shows lower shrinkage values. As for M1, samples based on sodium exhibit the lowest shrinkage values with a very low kinetic over 28 days. The shrinkage values at 28 days are about 1477, 297, and 141 µm/m for K^6M5, K^9M5, and Na^9M5 samples, respectively. This fact can be explained by the higher impurities content of M5 metakaolin such as quartz playing the role of a filler [38].

In order to highlight the effect of metakaolin and alkaline solution, the shrinkage values at 14 days were plotted in function of the aluminum and alkali cation concentrations (**Figure 5**). The aluminum concentration seems to have little influence on the shrinkage value (**Figure 5a**). Indeed, very different shrinkage values can be obtained for slightly different aluminum concentrations. For example, at similar concentration of aluminum (5.9 mol.L^{-1}), the shrinkage of K^9M1 is three times higher than Na^9M1. More changes can be observed in the function of the alkali cation concentration (**Figure 5b**). For the same metakaolin, the use of potassium alkaline solution with higher alkalinity (K^9 instead of K^6 solution) reduces the shrinkage value. For example, K^6M1 and K^9M1 mixtures have concentrations equal to 3.57

and 5.84 mol.L^{-1} and shrinkage values equal to 1350 and 1200 µm/m respectively. For mixtures based on M5, the shrinkage can be multiplied by 6 by changing the solution. A higher alkalinity of the alkaline solution induces a higher depolymerization degree leading to small species that are able to reorganize and react easily and more rapidly [39, 40]. However, the lower alkalinity of K^6 solution slows down the kinetics of the reaction. The continuous reorganization and rearrangement of geopolymer structure can also explain the increase of the shrinkage over time [41]. Furthermore, changing the cation K^+ by Na^+ permits to reduce the shrinkage considerably. This result can be explained by the difference between the two alkaline cations i.e the smaller cation size and the larger hydration sphere of Na^+ compared to K^+ cation [42]. In addition to that, it has been shown in previous work [38] that, for different metakaolins, K^6 solution leads to a higher porosity rate and smaller pore size of resulting geopolymers (0.01 µm) compared to K^9 (0.03 µm) and Na^9 (0.04-0.06 µm). This fact is also directly related to the shrinkage. Indeed, smaller pores lead to higher stresses and thus higher endogenous shrinkage [43].

Consequently, the preponderant impact of the alkaline solution (alkali type and concentration) on the geopolymerization rate and pore size distribution affects directly the endogenous shrinkage of geopolymers.

3. Impact of additives on the endogenous shrinkage

The influence of different additives on the endogenous shrinkage has been investigated. For this, two types of sand (normalized sand and sand), glass fiber and wollastonite were added to K^7M1 mixture. The evolution of shrinkage as a function of time is plotted in **Figure 6**. Without additive, K^7M1 sample shows a high increase in the shrinkage during the two first days. The shrinkage increases from 0 to 460 µm/m at 1 and 2 days respectively, and achieves 620 µm/m at 7 days. The addition of wollastonite decreases the shrinkage to 450 at 7 days (a reduction by 27.5% compared to sample without additive). The impact of glass fiber is more visible, especially at an early age. Indeed, the shrinkage value decreases to 76 and 350 µm/m at 2 and 7 days (a reduction by 43.6%). Moreover, the use of sand reduces the shrinkage to 250 µm/m at 7 days. The use of normalized sand shows the lowest shrinkage value at 7 days (142 µm/m, a reduction by 77.1%) which is comparable to mortar (182 µm/m at 7 days). Thus, all additives permit to reduce of the endogenous shrinkage to different extents. This fact suggests a modification of the granular skeleton and of the pore size distribution that reduce the tensile forces and the stresses causing the endogenous shrinkage [44].

In order to highlight the effect of additive on the microstructure and granular skeleton of geopolymers and to exacerbate the effect of free and physisorbed water release, in situ environmental SEM observations were performed with a variation of temperature from 25 to 300°C. The obtained micrographs at 25 and 300°C are presented in **Figure 7**. K^7M1 sample, without additive, shows a typical microstructure of metakaolin geopolymer with platy metakaolin particles [45]. At 300°C, a similar microstructure was observed. However, cracks can be noticed revealing shrinkage stresses caused by the release of free and physisorbed water. Sample with wollastonite K^7M1W, shows a similar microstructure indicating that the wollastonite is well dispersed in the matrix [46]. At 300°C, smaller cracks compared to sample without additives can be observed. The micrograph of $S3M1_{16}G$ sample demonstrates a low adhesion between the glass fiber and the geopolymer matrix. At 300°C, a glass fiber debonding is shown. In fact, the glass fibers can disrupt the interconnection of pores, reducing the water content in the capillary pore [47]. K^7M1S Sample shows a higher compact structure and spherical morphology characteristic of sand. Indeed, the sand increases the granular compactness of the skeleton. Spherical morphology characteristic of sand is observed. At 300°C, no visible cracks can be detected. K^7M1NS sample shows a geopolymer matrix and embedded sand particles. At 300°C, no variation is observed. Normalized sand modifies also the pore structure of the geopolymer [48]. The highest capacity of normalized sand to reduce the shrinkage can be explained by the modification of the granular skeleton decreasing hence the contraction forces. Furthermore, quartz is known to act as a rigid inert skeleton limiting the shrinkage [49].

Concerning the compressive strength (Table 1), no direct relation has been shown with the shrinkage. For the binders (without additives), the compressive strength values are governed by the alkaline solution. In fact, regardless of the used metakaolin, samples based on K6 solution present the lowest values compared to K^7, K^9 and Na^9 solution (32, 51, 60 and 70 MPa for K^6M1, K^7M1, K^9M1 and Na^9M1 samples , respectively). This is due to higher amount of reactive siliceous species in the higher alkali-concentrated solutions favoring the geopolymer network and reinforcing the structure [38]. The wollastonite or glass fibers act also as reinforcement and increase the compressive strength (70 and 90 MPa for K^7M1G and K^7M1W samples, respectively). However, the addition of sand does not influence significantly the compressive strength (58 and 53 for K^7M1S and K^7M1NS samples, respectively) [50].

The shrinkage at 7 days of all studied samples with or without additives was plotted in function of liquid to solid mass ratio (L/S) and the open porosity in **Figure 8.** Other formulations were also tested and added to the graph in order to validate the correlation. A general tendency shows the increase of the shrinkage with the increase of liquid to solid ratio. Geopolymer binders (without additives), except for K^9M5 and Na^9M5 samples, exhibit high liquid to solid ratios varying between 1.0 and 1.3 and high porosity values (about 35%) which corresponds to high shrinkage value ranging from 500 to 620 µm/m. These binders can be suitable for coating applications. Indeed, the high L/S ratio enables the spraying and favors interactions with different substrates. In the case of K^9M5 and Na^9M5 samples, the high alkalinity of the solution, the presence of quartz, and the higher median diameter of metakaolin M5 compared to metakaolin M1 can explain the lower values of the L/S ratio (about 0.6) and the porosity (about 29 %) and therefore the decrease of the shrinkage values (163 and 119 µm/m for K^9M5 and Na^9M5 samples respectively). The incorporation of additives (glass fiber, wollastonite, a mixture of both and sand) decreases the ratio to 0.20-1.17 but does not induce a major change in the open porosity (about 34%) which is accompanied by a decrease in the shrinkage values from 280 to 420 µm/m. These formulations can be used for additive manufacturing [51] and present a similar value of shrinkage when 3D a printing or casting process is used. The increase of sand proportion or the use of a mixture of glass fiber, wollastonite, and sand permits to reduce of the L/S ratio to 0.3-0.5 and the open porosity to about 24% inducing the decrease of the shrinkage between 200 and 100 µm/m. The lowest shrinkage values < 200 µm/m are obtained for NS based samples showing the lowest L/S ratio (about 0.2) and the lowest porosity (about 16%). This is due to the change of the granular skeleton as previously explained.

Consequently, the alkaline solution, the liquid to solid ratio, and the nature of additive are key parameters controlling the endogenous shrinkage of metakaolin based geopolymer.

II. CONCLUSION

The reduction of shrinkage of geopolymer materials remains a challenge in different application fields. The objective of this work is to provide a clearer insight into the impact of precursors and additives on the shrinkage of geopolymer materials. Different samples based on 4 alkaline solutions, 2 metakaolins, and 4 additives were synthesized and stored at 20°C and 100% HR. It was evidenced that there is no variation of mass of the samples over

time, which means that the shrinkage is endogenous, and caused by self-desiccation due to geopolymerization reaction. It is possible to propose an endogenous shrinkage mapping:

i) In the case of geopolymer binders (without additives), the increase of cation concentration or the use of sodium silicate solution lead to higher and faster geopolymerization rate inducing denser structure with higher pore size that decreases the endogenous shrinkage to less than 400 µm/m at 28 days. The compressive strength are governed by the alkaline solution and varies between 32 and 84 MPa.

ii) The addition of wolloatonite and /or glass fibers and sand permit to obtain a shrinkage varying from 280 to 420 µm/m. The compressive strengths are improved until 90 MPa with the addition of wollastonite.

In the case of geopolymer mortars, the use of normalized sand reduces considerably the shrinkage to 100 µm/m at 7 days, which can be explained by a modification of the granular skeleton and the pore size distribution. A conservation of the mechanical properties at 50 MPa was proven. A correlation has shown to increase the shrinkage with an increasing of liquid to solid ratio and open porosity

References

[1] J. Davidovits, Geopolymers and geopolymeric materials, J. Therm. Anal. 35 (1989) 429-441.

[2] J. Provis, Geopolymers and other alkali activated materials: why, how, and what? Mater. Struct. 47 (2014) 11–25.

[3] J. Davidovits, (2013), Geopolymer Cement a review, published in Geopolymer Science and Technics, Technical Paper #21, Geopolymer Institute Library, www.geopolymer.org.

[4] J. Davidovits, Geopolymer Chemistry and Applications, 2nd ed. Saint-Quentin, France : Institut Geopolymer, 2008.

[5] C. Dupuy, A. Gharzouni, N. Texier-Mandoki, X. Bourbon, S. Rossignol, Thermal resistance of argillite-based alkali-activated materials. Part 1: Effect of calcination processes and alkali cation, Mater. Chem. Phys. 2173 (2018) 23-333.

[6] J.L. Provis, J. S J Van Deventer, Geopolymers. Structure, Processing, Properties and Industrial Applications, Woodhead Publishing Limited, 2009.

[7] P. Duxson, A. Fernandez-Jimenez, J.L. Provis, G.C. Lukey, A. Palomo, J.S.J. Van Deventer, Geopolymer technology : the current state of the art, J. Mater. Sci. 42 (2007) 2917-2933.

[8] F. Collins, JG. Sanjayan, Cracking Tendency of Alkali-Activated Slag Concrete Subjected to Restrained Shrinkage, Cem. Concr. Res. 30 (2000) 791-798.

[9] G. W. Scherer Drying, shrinkage, and cracking of cementitious materials, Transp. Porous Media. 110 (2015) 311-331.

[10] J.M. Reynouard, G. Pijaudier-Cabot, Comportement mécanique du béton, Mécanique Ingénierie Matériaux, Hermes science publication, 2005.

[11] L. Wu, N. Farzadnia, C. Shi, Z. Zhang, Autogenous shrinkage of high performance concrete : a review, Constr. Build. Mater. 149 (2017)62-75,

[12] A. Li, S. Zhang, Y. Zuo, W. Chen, G. Ye, Chemical deformation of metakaolin based geopolymer, Cem. Concr. res.120 (2019) 108-118.
[13] C. Kuenzel, L.J. Vandeperre, S. Donatello, A. R. Boccaccini, C. Cheeseman, Ambient temperature drying shrinkage and cracking in metakaolin-based geopolymers, J. Am. Ceram. Soc. 95 (2012) 3270-3277.
[14] A. Hawa, D. Tonnayopas, W. Prachasaree, Performance evaluation and microstructure characterization of metakaolin-based geopolymer containing oil palm ash, Sci. World J. 2013 (2013) 9.
[15] R. Si, Q. Dai, S. Guo, J. Wang, Mechanical property, nanopore structure and drying shrinkage of metakaolin-based geopolymer with waste glass powder, J. Clean. Prod. 242 (2020) 118502
[16] C. Kuenzel, L. Li, L. Vandeperre, A.R. Boccaccini, C.R. Cheeseman, Influence of sand on mechanical properties of metakaolin geopolymers, Constr. Build. Mater. 66 (2014) 442-446.
[17] S. Riahi, A. Nemati, A.R. Khodabandeh, S. Bagshahi, The effect of mixing molar ratios and the sand particles on microstructure and mechanical properties of metakaolin-based geopolymer, Mater. Chem. Phys. 240 (2020) 122223.
[18] T. Yang, H. Zhu, Z. Zhang, Influence of fly ash on the pore structure and shrinkage characteristics of metakaolin-based geopolymer pastes and mortars, Constr. Build. Mater. 153, (2017) 284-293.
[19] H. Hyodo, M. Tanimura, R. Sato, K. Kawai, Evaluation of effect of aggregate properties on drying shrinkage of concrete, The Third International Conference on Sustainable Construction Materials and Technologies, Kyoto, Japan, 2013.
[20] K. Sagoe-Crentsil, T. Brown, A. Taylor, Drying shrinkage and creep performance of geopolymer concrete, Journal of Sustainable Cement-based Materials, 3 (2013) 35-42.
[21] L.P. Qian, Y.S. Wang, Y. Alrefaei, J.G. Dai, Experimental study on full-volume fly ash geopolymer mortars: sintered fly ash versus sand as fine aggregates, J. Clean. Prod. 263(2020) 121445.
[22] Y. Wang, C. L. Chan, S.H. Leong, M. Zhang, Engineering properties of strain hardening geopolymer composites with hybrid polyvinyl alcohol and recycled steel fibres, Constr. Build. Mater.261 (2020) 120585.
[23] A.A. Melo Neto, M.A. Cincotto, W. Repette, Drying and autogeneous shrinkage of pastes and mortars with activated slag cement, Cem. Concr. Res. 38 (2008) 565-574.
[24] X. Yao, T. Yang, Z. Zhang, Compressive strength development and shrinkage of alkali-activated fly ash-slag blend associated with efflorescence, Mater. Struct. 49 (2015) 1-12.
[25] P.S. Deb, P. Nath, P.K. Sarker, Drying shrinkage of slag blended fly ash Geopolymer concrete cured at room temperature, Procedia Engineering 125 (2015) 594-600.
[26] C. Sun, J. Xiang, M. Xu, Y. He, Z. Tong, X. Cui, 3D extrusion free forming of geopolymer composites: materials modification and processing optimization, J. clean. Prod. 258 (2020)120986.
[27] L. Yang, Z.J. Jia, Y.M. Zhang, J.G. Dai, Effects of nano-TiO_2 on strength, shrinkage and microstructure of alkali activated slag pastes, Cem. Concr. Compos. 57 (2015) 1-7.
[28] M. Kheradmand, Z. Abdollahnejad, F. Pacheco-Torgal, Drying shrinkage of fly ash geopolymeric mortars reinforced with polymer hybrid fibres, Construction Materials, 173 (2020) 28-40
[29] K. Mermerdas, Z. Algin, S. Ekmen, Experimental assessment and optimization of mix parameters of fly ash-based lightweight geopolymer mortar with respect to shrinkage and strength, J. Build. Eng. 31 (2020) 101351.

[30] B. Behforouz, V.S. Balkanlou, F. Naseri, E. Kasehchi, E. Mohseni, T. Ozbakkaloglu, Investigation of eco-friendly fiber-reinforced geopolymer composites incorporating recycled coarse aggregates, Int. J. Environ. Sci. 17 (2020) 3251-3260.
[31] R. Si, Q. Dai, S. Guo, J. Wang, Mechanical property, nanopore structure and drying shrinkage of metakaolin-based geopolymer with waste glass powder, J. Cleaner Prod. 242 (2020) 118502.
[32] C. Dupuy, A. Gharzouni, I. Sobrados, N. Tessier-Doyen, N. Texier-Mandoki, X. Bourbon, S. Rossignol, Formulation of an alkali-activated grout based on Callovo-Oxfordian argillite for an application in geological radioactive waste disposal, Constr. Build. Mater. 232 (2020)117170.
[33] S. Petlitckaia, A. Poulesquen, Design of lightweight based geopolymer foamed with hydrogen peroxide, Ceram. Int. 45 (2019) 1322-1330,.
[34] C. Dupuy, A. Gharzouni, N. Texier-Mandoki, X. Bourbon, S. Rossignol, Thermal resistance of argillite-based alkali-activated materials. Part 1: Effect of calcination processes and alkali cation, Mater. Chem. Physics. 217 (2018) 323-333,.
[35] E. Najafi and A. Allahverdi, Investigating shrinkage changes of natural pozzolan based geopolymer cement paste, Iran. J. Mater. Sci. Eng. 8 (3) (2011) 50-60.
[36] A. A. M. Neto, M. A. Cincotto, W. Repette, Drying and endogenous shrinkage of pastes and mortars with activated slag cement, Cem. Concr. Res. 38(4) (2008) 565-574.
[37]D.S. Perera, E.R. Vance, K.S. Finnie, M.G. Blackford, J.V. Hanna, D.J. Cassidy, C.L. Nic holson, Disposition of water in metakaolinite-based geopolymers, Ceram. Trans.185 (2005) 225-236
[38] A. Gharzouni, I. Sobrados, E. Joussein, S. Baklouti, S. Rossignol, Predictive tools to control the structure and the properties of metakaolin based geopolymer materials, Colloid. Surf.A A. 511(2016) 212-221.
[39] L.B. Jonathan, L.T. Garry, Anion distributions in sodium silicate solutions. characterization by ^{29}Si NMR and infrared spectroscopies, and vapor phase osmometry, J. Phys. Chem. B, 101 (1997) 10638-10644
[40] A. Gharzouni, E. Joussein, B. Samet, S. Baklouti, and S. Rossignol, Effect of the reactivity of alkaline solution and metakaolin on geopolymer formation, J. Non. Cryst. Solids. 410 (2015) 127–134.
[41] G. Fang, H. Bahrami, M. Zhang, Mechanisms of endogenous shrinkage of alkali-activated fly ash-slag pastes cured at ambient temperature within 24 h, Constr. Build. Mater. 171 (2018) 377-387.
[42] J. Mähler, I. Persson, A study of the hydration of the alkali metal ions in aqueous solution, Inorg. Chem. 51 (2012) 425-438
[43]A.R. Sakulich, D.P. Bentz, Mitigation of endogenousshrinkage in alkali activated slag mortars by internal curing. Mater. Struct. 46 (2013) 1355–1367. https://doi.org/10.1617/s11527-012-9978-z
[44] K.Liu, R. Yu, Z. Shui, S. Yi, X. Li, G. Ling, Y. He, Influence of external water introduced by coral sand on endogenous shrinkage and microstructure development of Ultra-High Strength Concrete (UHSC), Constr. Build. Mater. 252 (2020) 119111.
[45] J. Temuujin, A. Minjigmaa, W.Rickard, M. Lee, I. Williams, A. van Riessen, Preparation of metakaolin based geopolymer coatings on metal substrates as thermal barriers, Appl. Clay Sci. 46 (2009) 265-270.
[46] J. Archez, N. Texier-Mandoki, X. Bourbon, J.F. Caron, S. Rossignol, Influence of the wollastonite and glass fibers on geopolymer composites workability and mechanical properties, Constr. Build. Mater. 257 (2020) 119511.

[47] F.Ullah, F. Al-Neshawy, J. Punkki, Early Age Endogenous Shrinkage of Fibre Reinforced Concrete, Nord. Concr. Res. 59 (2018) 59-72. 10.2478/ncr-2018-0015.
[48] F. Colangelo, G. Roviello, L. Ricciotti, C. Ferone and R. Cioffi, Preparation and Characterization of New Geopolymer-Epoxy Resin Hybrid Mortars, Materials 6(7) (2013) 2989-3006. https://doi.org/10.3390/ma6072989
[49] S. Campopiano, A. Iadicicco, F. Messina, C. Ferone, R. Cioffi, Fiber Bragg grating sensors as a tool to evaluate the influence of filler on shrinkage of geopolymer matrices. Optical Sensors 2015. (2015) doi:10.1117/12.2182343
[50] X. Li, F. Rao, S. Song, M.A. Corona-Arroyo, N. Ortiz-Lara, E.A. Aguilar-Reyes, Effects of aggregates on the mechanical properties and microstructure of geothermal metakaolin-based geopolymers, Results in Physics, 11, 267-273 (2018) doi.org/10.1016/j.rinp.2018.09.018.
[51] J. Archez, N. Texier-Mandoki, X. Bourbon, J.F. Caron and S. Rossignol, Adaptation of the geopolymer composite formulation to the shaping process. Mater. Today Commun.25 (2020) 101501. https://doi.org/10.1016/j.mtcomm.2020.101501.

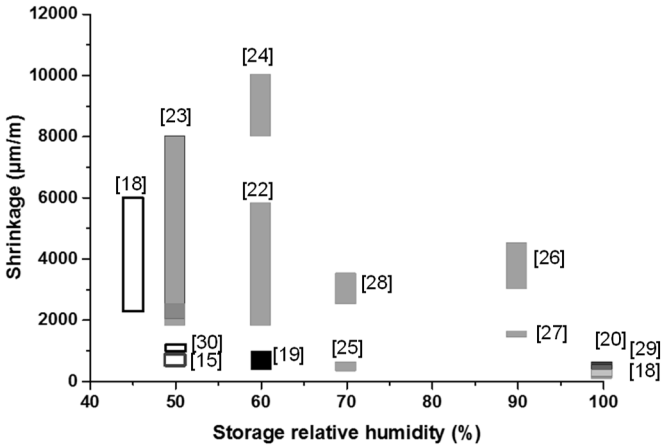

Figure 1. Examples of shrinkage values from literature in function of relative humidity storage conditions for (■) concrete, (■) alkali activated materials and (□) geopolymers.

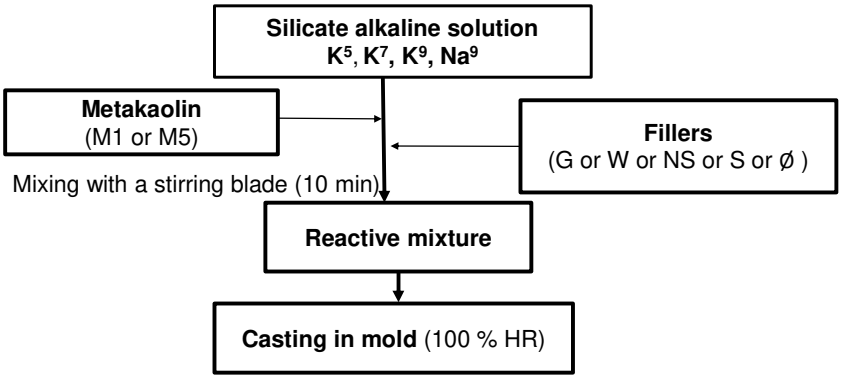

Figure 2. protocol used to synthesize and store geopolymers.

(a) **(b)**

Figure 3. Photo (a) of the shrinkage measurement and (b) of the sample storage in sealable plastic bag

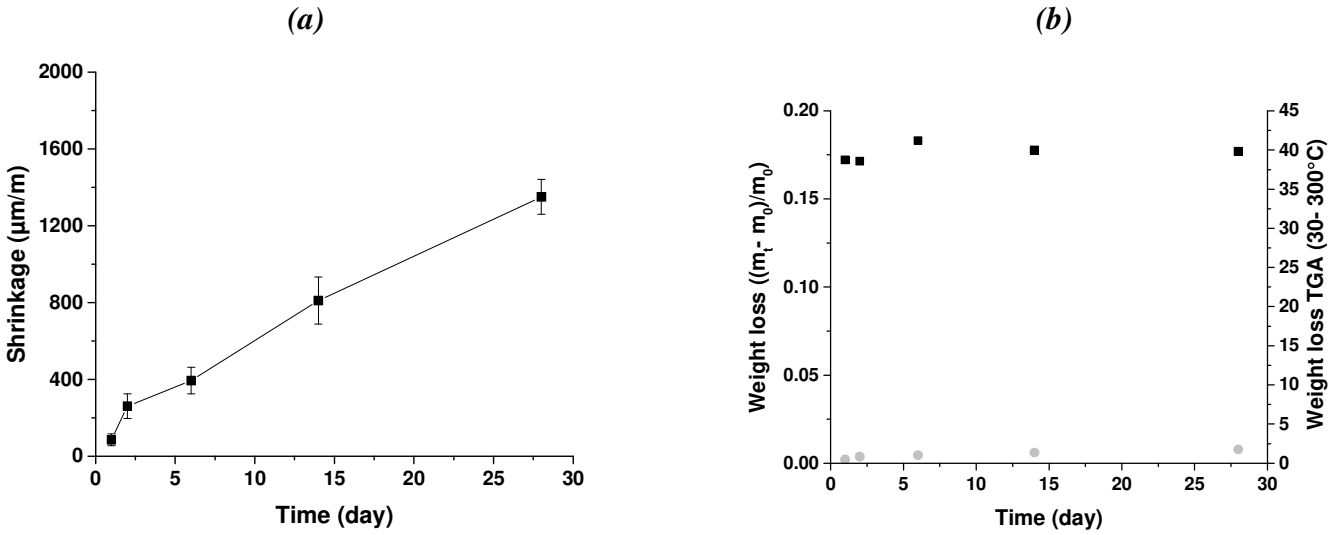

Figure 4. **(a)** Shrinkage as function of time and **(b)** weight loss ($\frac{mt-m0}{m0}$) measured with (●) a balance and (■) with TGA analysis (30-300 °C) as a function of time for K^6M1 sample stored at 100 % RH.

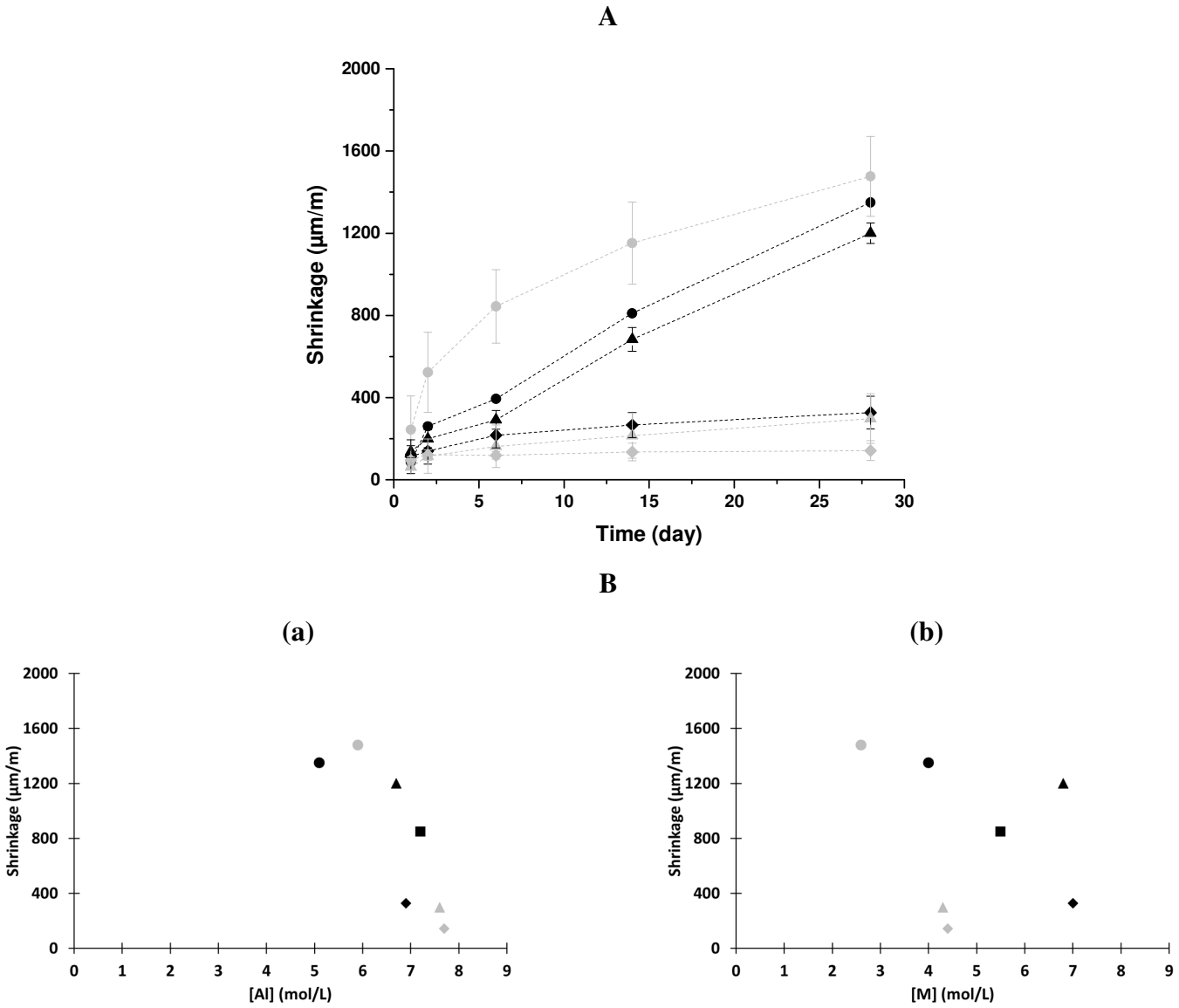

Figure 5. (A) Shrinkage evolution as a function of time for the compositions (●) K^6M1, (▲) K^9M1, (◆) Na^9M1, (●) K^6M5, (▲) K^6M5, (◆) Na^9M5 and (**B**) shrinkage at 28 days as a function of **(a)** aluminum [Al] and **(b)** alkali concentrations [M] (M=K or Na) for the composition (●) K^6M1, (▲) K^9M1, (■) K^7M1 (◆) Na^9M1, (●) K^6M5, (▲) K^9M5 and (◆) Na^9M5.

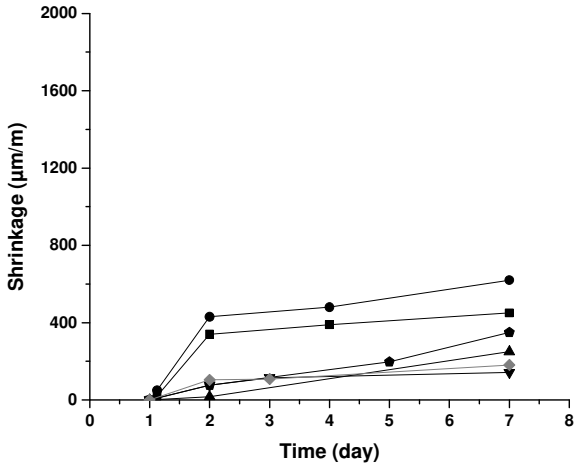

Figure 6. Shrinkage evolution as a function of time for the compositions based on different additives (●) K^7M1 (■) K^7M1W (⬟) K^7M1G (▲) K^7M1S (▼) K^7M1NS and for (◆) mortar.

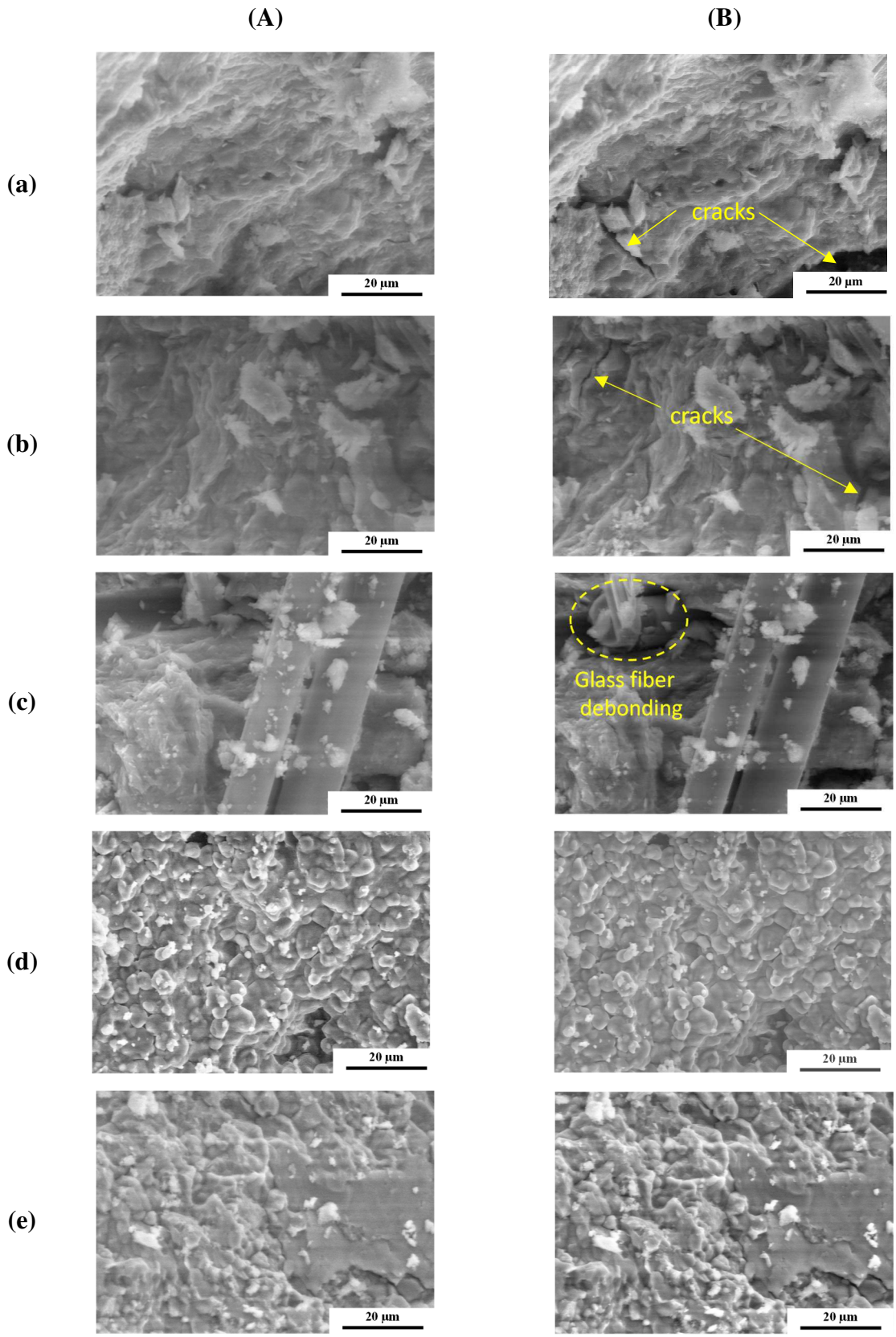

Figure 7. SEM micrographs at **(A)** 25 and **(B)** 300°C of **(a)** K^7M1 **(b)**, K^7M1W **(c)**, K^7M1G **(d)** K^7M1S and **(e)** K^7M1NS.

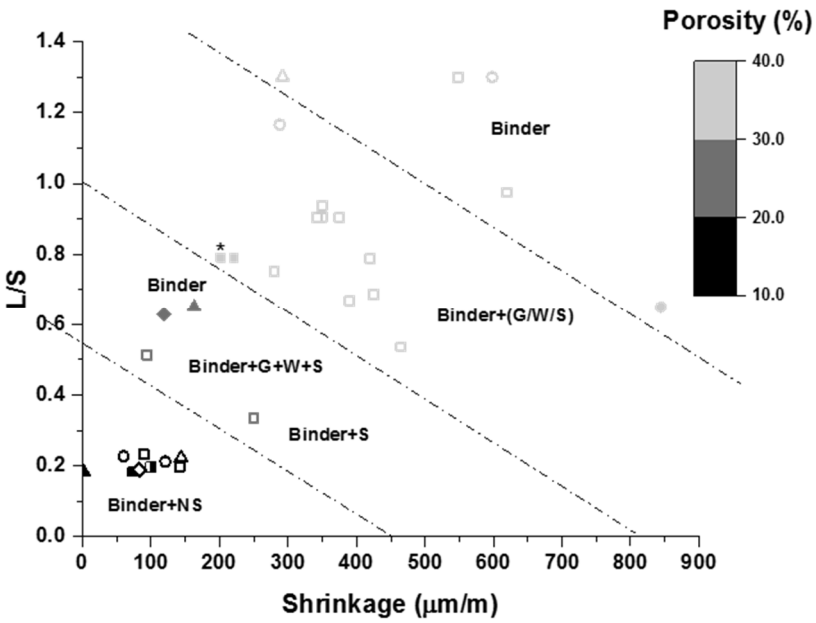

Figure 8. Evolution of the shrinkage at 7 days of the different studied sample in function of the liquid to solid ratio (L/S) and porosity (* made by additive manufacturing).

Table 1: Chemical composition and compressive strength of the studied samples

Sample	L/S	Additives (wt.%)				Molar ratios		σ (± 4 MPa)	Density
		W	G	S	NS	K_2O/SiO_2	K_2O/Al_2O_3		
K^6M1	1.30					0.26	0.74	32	1.57
K^9M1	1.30					0.33	1.01	60	1.76
Na^9M1	1.30					0.29	1.01	70	1.75
K^6 M5	0.65					0.17	0.42	50	1.72
K^9M5	0.65					0.24	0.62	78	1.90
Na^9M5	0.63					0.22	0.63	84	1.86
K^7M1	0.97					0.25	0.59	71	1.64
K^7M1NS	0.23				66	0.25	0.59	55	2.27
K^7M1S	0.53			29		0.25	0.59	45	1.93
K^7M1G	0.94		2			0.25	0.59	70	1.82
K^7M1W	0.75	15				0.25	0.59	90	1.80